EVALUATION OF FORMATION FLIGHTS WITH LONG RANGE AIRCRAFT FOR DIFFERENT FLIGHT CONDITIONS AND ATMOSPHERIC DISTURBANCES

C. Zumegen*, T. Marks†, E. Stumpf*

* RWTH Aachen University, Institute of Aerospace Systems, Wüllnerstr. 7, 52062 Aachen, Germany
† German Aerospace Center (DLR), Air Transportation Systems, Blohmstraße 20, 21079 Hamburg, Germany

Abstract

The aerodynamic formation flight, which is also called air wake surfing for efficiency (AWSE), can lead to a high drag reduction at the trailing aircraft of more than ten percent resulting in a reduced fuel burn. Therefore, this operational strategy represents a promising means to reduce the greenhouse effect of aviation. The following study investigates the flight of two long haul commercial aircraft in an echelon formation in a stationary state, a flight dynamic simulation and finally at trajectory level. Thereby, the effect of different cruise altitudes and speeds, aircraft masses, lateral and vertical separations and different intensities of gusts and turbulence are evaluated. Based on the aircraft data set from the in house preliminary aircraft design tool MICADO a vortex lattice method calculates the induced loads in the trailing wake behind the leader. Subsequently, the results are used in the flight simulation program to analyze the flight behavior of the trailing aircraft in the formation under the influence of atmospheric disturbances. Finally, the results of the vortex lattice method and the flight simulation provide the necessary input data for the evaluation of the benefits achievable during the entire mission based on a detailed trajectory calculation. High altitudes and low Mach numbers during the formation flight lead to the highest drag reductions at the trailing aircraft. Movements of the trailing aircraft away from the optimum location in the vortex of the leading aircraft and additional detours lead to reduced fuel savings of ten percent or less.

Keywords

Air wake surfing for efficiency; Vortex Lattice method; Flight simulation; Trajectory calculation

1. INTRODUCTION

According to the International Council on Clean Transportation (ICCT), the CO_2 emissions in the aviation industry increased by 32% between 2013 and 2018. In 2018, the amount of CO_2 emissions represented 2.4% of the global CO_2 emissions of the fossil fuel burned [1]. This is in strong contrast to the goals formulated in the CORSIA document by the International Civil Aviation Organization (ICAO), which aim to stabilize the net CO_2 emissions in the aviation industry after 2020 and to reduce the net CO_2 emissions by 50% in 2050 [2]. In order to reverse this trend, formation flight (air wake surfing for efficiency; AWSE) can be a promising approach to mitigate the influence of the aviation industry on the global warming.

During the formation flight, the pressure difference between the upper and lower side of the leading aircraft wing creates a compensating flow, which induces a vortex at both wing tips. A trailing aircraft can fly in the up wash field of one of these vortices to benefit from the energy of the trailing vortex like a surfer in a wave. The up wash field in the vortex requires to pitch the aircraft downwards by the angle γ_a in figure 1 to maintain a constant altitude. At a stationary flight state, the tilted weight vector W leads to a reduced thrust T. [3]

Since the attitude of the trailing aircraft in the following investigation is constant, only the angle of attack changes in the up wash field. In that way, the new angle of attack can reduce the drag of the trailing aircraft.

Motivated by the formation of migrating birds,

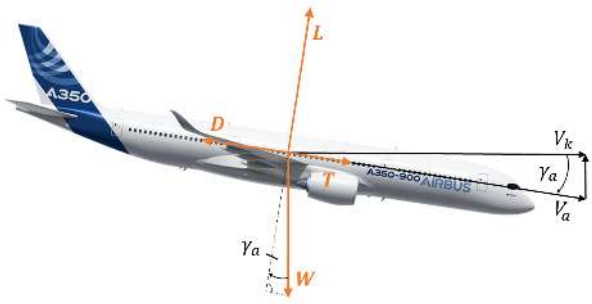

FIG 1. Principle of air wake surfing for efficiency (AWSE) [3]

doi:10.25967/530159

Beukenberg and Hummel set up flight experiments to investigate the power reduction of the trailing aircraft in a formation of two Do-28 aircraft, which led to power reductions of about 15%. [4] Later on, this effect was investigated for larger aircraft by the NASA Dryden Research Center. The formation flight of two C-17 Globmaster III at a constant altitude and speed of 25000 ft and 275 kts showed a drag reduction of approximately 7% to 8% compared to reference locations outside of the influence of the leading aircraft vortex. During the experiment, the stream wise separation distance between the two aircraft varied between 1000 ft and 3000 ft, which is equal to 6 and 18 times the aircraft span. Due to high velocity gradients at a close distance to the vortex core, the pilot had difficulties in flying at the optimum region behind the leading aircraft. Nevertheless, the energy consumption decreased. [5]
A current announcement of Airbus in 2019 shows that the principle of AWSE is an ongoing subject of research. Aiming at a fuel reduction of five to ten percent Airbus wants to investigate the potential energy savings of two Airbus A350 in formation flight. [6]
In order to predict the benefits of formation flights on different flight routes, this paper will investigate the drag reduction of two long-haul aircraft in formation flight at different flight conditions. Additionally, the alleviation of the benefits due to atmospheric disturbances will be considered. At first, the selected input parameters for the simulation are presented in chapter 2. Subsequently, chapter 3 explains the methods and the integrated tools before the results are shown in chapter 4. In chapter 5, a conclusion will be given.

2. GENERAL APPROACH

In order to perform formation flights, a minimum of two aircraft need to fly on the same route and the same time. This requires diversions on the flight path and additional planning, which is related to additional costs and emissions. Due to these constraints, long distance flights are most likely to overcome the additional expenses. Figure 2 presents commercial aircraft families with a design range of more than 5000 nm. To include future developments ordered aircraft are also taken into account. The diagram shows that the number of modern two engine wide body aircraft will increase the most in the future. In particular, these are the Airbus A330 and A350 families as well as the Boeing B777 and B787 families. Therefore, the A330-200, the A350-900, the B777-200 and the B787-8 are further investigated in this paper. Since formation flight requires a high synchronization effort between the aircraft, only two aircraft are considered to fly in formation.
The selected aircraft will perform formation flights at different flight levels and flight velocities. Furthermore, the aircraft masses change during flight due to the fuel consumption. In the simulations the velocity

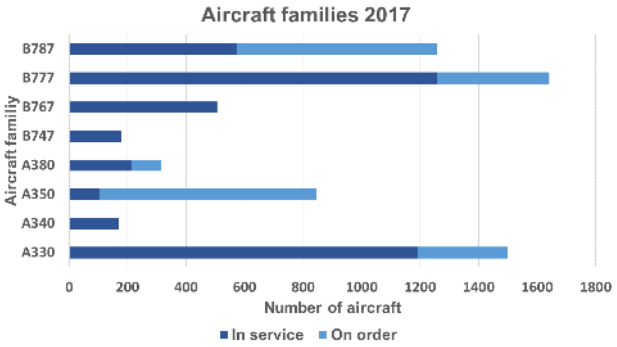

FIG 2. Number of orders and aircraft in service [7]

ranges from 0.78 to the maximum operating mach number. The upper limit of the flight altitude is set by the maximum operating altitude, whereas 35000 ft is the lowest altitude in the simulations. The maximum altitude and speed of a formation pair is set by the aircraft with the lower limit. Because the trajectory calculation module uses an optimization method for the flight trajectory, the aircraft mass varies between a large range of $0.9 \cdot OME$ (operating mass empty) and $1.1 \cdot MTOM$ (maximum take-off mass).
The geometry of the formation in the simulation is characterized by the stream wise, lateral and vertical distance between to the two participating aircraft. Whereas the stream wise distance Δx in figure 3 is measured between the nose of the two aircraft, the lateral and vertical distance is set by the longitudinal axis of the two aircraft. The lateral distance Δy is calculated by the half span of the leading aircraft and the trailing aircraft, which is multiplied by a lateral separation factor k_y.
The vertical distance Δz in figure 4 is the product of

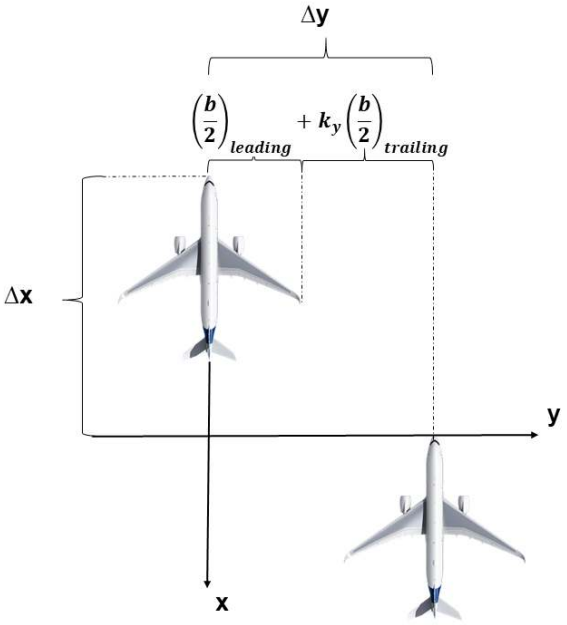

FIG 3. Horizontal separation of the aircraft

the vertical separation factor k_z and the half span of the trailing aircraft.

If the participants of the formation fly with a small

FIG 4. Vertical separation of the aircraft

stream wise distance, ice and loose aircraft parts of the leading aircraft or a collision between the formation partners raise serious safety concerns. Hence, the stream wise distance is set to 30 times the trailing aircraft span. At this distance, the initial vortex sheet behind the wing of the leading aircraft is completely rolled up, leading to two trailing, counter rotating vortex pairs. In the work of Ning, Flanzer and Kroo the aerodynamics of extended formation flights with a stream wise distance of ten times the aircraft span and more were investigated. Their analysis include the effects of wake roll up, viscous decay, vortex instabilities and vortex propagation due to induced velocities and stratification. The wake roll up model was based on an approach of Betz and Donaldson [8] [9], which provided the initial condition for the viscous wake decay afterwards. The drag savings for different vertical and lateral positions of the trailing aircraft, which flies ten spans behind the leading aircraft, is shown in figure 5. When the wing tips of the leading and trailing aircraft are aligned, the vertical and lateral distance is zero. [10]

As the vortex core sinks downward and moves

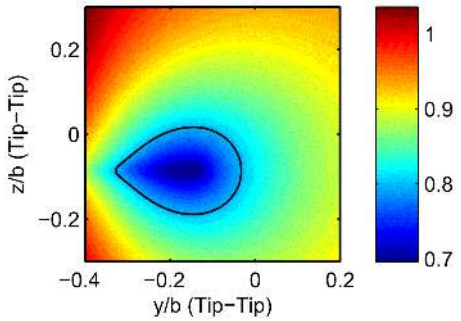

FIG 5. Induced drag savings at a streamwise distance of ten spans [10]

inboards, the highest drag reduction is not found at lateral and vertical distance of zero. Flight test showed, that the radius of the vortex core is constant up to a stream wise distance of approximately 200 spans behind the aircraft [11]. Afterwards, a rapid decay of the vortex occurs. Therefore, the results of Ning should be valid at a distance of 30 spans behind the leading aircraft as well. Hence, the lateral and vertical separation factors k_y and k_z varies between 0.6 and 1.4 or -0.4 and 0.4 in the simulation.

Table 1 presents the input parameters and their ranges.

Parameter	Lower limit	Upper limit
flight altitude	35,000 ft	Maximum operating altitude
flight Mach number	0.78	Maximum operating Mach number
leading aircraft mass	0.9 OME	1.1 MTOM
trailing aircraft mass	0.9 OME	1.1 MTOM
lateral separation factor	0.6	1.4
vertical separation factor	-0.4	0.4
streamwise separation	30 trailing aircraft spans	

TAB 1. Input parameters of the vortex lattice method and the flight simulation program

3. METHODS

The simulation process in figure 6 consists of three steps in order to obtain the average drag savings of a trailing long-haul commercial aircraft in formation flight. Initially, the aircraft data set, which is generated in the preliminary aircraft design tool MICADO (Multidisciplinary Integrated Conceptual Aircraft Design and Optimization) of the Institute of Aerospace Systems [12], is used to create the input file for the Athena Vortex Lattice Method (AVL). Hence, AVL can calculate the induced loads at the trailing aircraft in a formation. The drag of the reference case outside of the formation is saved in the Base Drag Database (BDD), whereas the induced loads at the trailing aircraft in formation can be found in the Drag Reduction Database (DRD). In the following step, the results from AVL are included in the flight simulation program JSBSim. Additional models of the atmospheric disturbances in JSBSim allow to calculate the reduced drag savings of the trailing aircraft under the influence of discrete gusts and continuous turbulence. The results of AVL and JSBSim are saved in the Turbulence Influence Database (TID). Finally, the Trajectory Calculation uses the BDD, the DRD and the TID to calculate the drag savings of an optimized flight trajectory.

3.1. Vortex lattice method

In order to use AVL, an additional tool has been implemented. This tool translates the geometry of the aircraft data set to the program AVL to calculate the induced drag and determines the additional aerodynamic drag due to viscous and transonic effects in a drag module of the preliminary design tool MICADO. The tool was developed in the dissertation of Yaolong Liu and has been validated with theoretical results and experiments in wind tunnels, which have shown a good agreement between the different methods. [13] In the AVL code, which was written by Mark Drela and Harold Youngren at the MIT, the lifting surfaces of an aircraft are discretized into panels in the stream- and

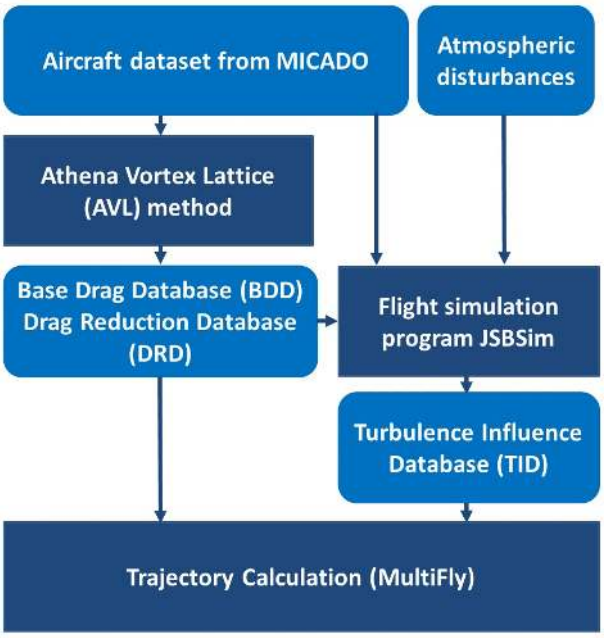

FIG 6. Simulation process

span wise direction. Thus, a distribution of horseshoe vortices can calculate the aerodynamic loads of the lifting surfaces and their trailing wakes. This method is limited to thin profiles and small angles of attack and sideslip and cannot capture flow separation. In a stationary cruise flight, which is investigated in this study, this limitation should not affect the results. A Prandtl-Glauert correction for compressibility effects takes the transonic flow at the lifting surfaces during the cruise flight into account. AVL can also consider slender bodies, such as fuselages, but their results are not well validated. Therefore, only the wing, the horizontal and vertical tail are included in AVL. Figure 7 shows the geometry of an Airbus A330-200 in AVL. The fuselage section of the wing is replaced by a rectangular surface. [14]

At first, AVL calculates only the leading aircraft to

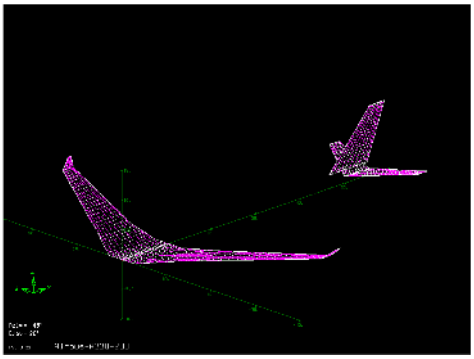

FIG 7. Airbus A330-200 in AVL

obtain the required angle of attack of the leader in cruise flight. Then, the whole formation is loaded into AVL and the induced drag, rolling and yaw moment at the trailing aircraft are analyzed. Afterwards, empirical and semi-empirical methods in the drag module of MICADO determine the viscous and the wave drag of the trailing aircraft.

To shorten the calculation time, the tool was parallelized by OpenMP [15]. This enables the calculation of various flight conditions of one formation on different processor cores. Afterwards, the tool was able to run on the RWTH Aachen University compute cluster to calculate the DRD of one formation pair in less than one day.

3.2. Dynamic flight simulation

The simulation program JSBSim includes the induced loads from AVL, a model for atmospheric disturbances and a simplified autopilot. To simulate the flight behavior of the trailing aircraft in formation flight, JSBSim needs a flight dynamic model of the aircraft. This model is created by the aircraft data set from MICADO and the program DATCOM+ Pro, which uses a collection of equations and methods called DATCOM and is able to estimate the stability and control of manned aircraft. [16] One advantage is its easy integration in the implemented tool. On the other hand, DATCOM+ Pro can only calculate one control surface of one type (e.g. aileron) at once and is not able to calculate the derivatives of vertical control surfaces. Due to the complex flow behavior in transonic and separated flow, the program has difficulties in predicting the derivatives at this flow conditions. [17]

From the results from DATCOM+ Pro JSBSim can create a non-linear six degree of freedom flight dynamics model. A maneuver script file contains the main events during the simulation, such as the initial trim process and the integration of the induced loads in formation flight and the atmospheric disturbances. At each time step during the simulation, the resulting forces and moments are summed up to calculate the change of the attitude and position of the aircraft. At the beginning of the simulation, the induced drag and induced rolling and yaw moment are interpolated from the results of AVL using the initial flight state (flight speed, flight altitude, aircraft mass) in order to create look-up tables for different positions of the trailing aircraft. To avoid errors due to the different methods for the determination of the induced drag in JSBSim and in AVL, JSBSim calculates the relative change of the induced drag in formation flight $\Delta C_{D,ind}$. The values for $C_{D,ind,formation}$ and $C_{D,ind,solo}$ are interpolated from the BDD and DRD.

$$\Delta C_{D,ind} = C_{D,ind,formation} - C_{D,ind,solo} \quad (1)$$

The atmospheric disturbances can occur in form of discrete gusts and continuous turbulence. The corresponding models, which are integrated in JSBSim, are based on the military specification “MIL-F-8785C” [18]. The turbulence model uses the

Dryden spectrum and requires the wind speed 20 ft above ground level and the probability of exceedance. Table 2 lists the three degrees of turbulence levels that are linked to the classification in “MIL F 8785C”.

The discrete gusts have a $1 - cos$ shape and are

Turbulence degree	Wind speed at 20 ft GRD (fps)
1	25.0
2	50.0
3	75.0

TAB 2. Turbulence levels

described by a ramp up, a constant phase and a decay of the velocity value. Whereas the duration for the three sections is constantly one second, the magnitude is varied for different gust degrees according to table 3.

In order to keep the trailing aircraft at the optimum

Gust degree	Gust magnitude (fps)
1	10.0
2	20.0
3	35.0

TAB 3. Gust levels

lateral and vertical distance to the leading aircraft, a simplified autopilot function is integrated in the JSBSim simulation. The function consists of an altitude hold for the vertical movement and a position hold for the lateral movement. For the altitude hold the difference between the initial and the current altitude is sent to a PID controller, which emits the necessary elevator deflection η_{ap} to keep the initial altitude. On the other hand, the position hold shall keep the aircraft at the optimum lateral position. To determine the required aileron deflection ξ_{ap}, the position hold consists of two PID controllers. The first one takes the lateral distance to the initial position $k_{y0} - k_y$ to calculate the required rolling angle Φ_{cmd}, where k_y is the lateral separation factor. The second PID controller transfers the commanded rolling angle Φ_{cmd} into the necessary aileron deflection ξ_{ap}. Figure 8 illustrates the applied autopilot structure.

The coefficients K_P, K_I, K_D of the PID controllers

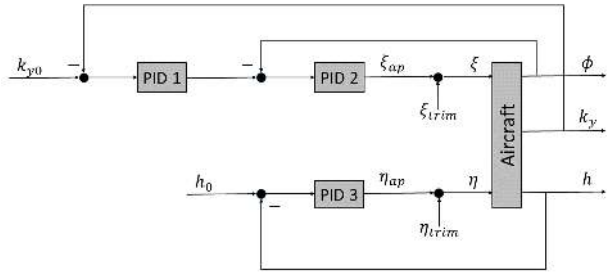

FIG 8. Simplified autopilot structure

are estimated with the tuning method by Chien, Hrones and Reswick [19]. For this method the step response of the flight condition parameters h, k_y and Φ_{cmd} to the control output (η_{ap}, ξ_{ap},Φ_{cmd}) is investigated. The step of the control output, normally the sudden deflection of one control surface, leads to a change of the aircraft attitude and position. If the deflection is constant, the natural stability of the aircraft leads to a reverse movement. Hence, an extreme attitude or position exists. The magnitude of the step, as well as the magnitude of the response and their temporal progression can be taken to tune the PID controllers.

A simulation of five minutes is performed for each initial flight condition (altitude, velocity, aircraft mass). After 20 seconds, the induced loads from the leading aircraft act on the aircraft. The simulation assumes the initial position of the trailing aircraft at the optimum position in the trailing vortex of the preceding aircraft. Afterwards, the induced loads are taken from the generated look-up tables for different lateral and vertical separation factors k_y and k_z. After 60 seconds, atmospheric disturbances in form of gusts and / or turbulence are included in the simulation. Finally, the average drag in formation flight between 100 and 400 seconds is determined for each gust and turbulence level. The ratio of the average drag and the drag before the start of the formation, at 19.5 seconds, is saved in the Turbulence Influence Database (TID).

3.3. Trajectory calculation

In order to assess the fuel saving benefit, the BDD and DRD are used to estimate the thrust reduction during the AWSE part of a formation. Here, a calculation of the trajectories of the leader and the follower is performed that is based on the Trajectory Calculation (MultiFly). This tool uses a total-energy model in combination with aircraft performance data (Base of Aircraft Data; BADA 4.2) from EUROCONTROL to solve the flight mechanical equations of motion (see [20] and [21]). The vortex strength of the leader’s wake depends on its flight state and weight. Therefore, the leader’s trajectory is calculated in a first step and subsequently used during the calculation process of the follower to account for the AWSE benefits. The leader’s state is accordingly interpolated at the current follower’s position. Additionally, the previously calculated databases are being used to assess the thrust reduction of the follower depending on the leader’s and follower’s masses as well as on altitude, speed and the follower’s position in the vortex using the Kriging interpolation method.

The influence of turbulence and gust is applied stochastically during the trajectory calculation process. Here, for a selected five minute interval the corresponding reduction of the benefits is interpolated from the TID and the benefit of the follower is reduced

accordingly for the time interval.

4. RESULTS

The evaluation of the benefits of formation flight is performed in three steps.
At first, the changed drag at the trailing aircraft in stationary state is investigated. The Vortex Lattice method AVL calculates the drag and induced moments at the trailing aircraft in formation and saves the results in the DRD. In order to measure the changed drag, the drag in the DRD is divided by the drag of the reference case with no leading aircraft in the BDD.
Subsequently, a simulation of the trailing aircraft in formation determines the average drag under influence of turbulence and gusts. The induced loads of the leader and the atmospheric disturbances change the position of the trailing aircraft in the vortex behind the leading aircraft and hence the drag. After the simulation, the averaged drag over five minutes flight time in formation is divided by the drag before the start of the influence of the formation and the atmospheric disturbances and saved in the TID. A ratio below one means that drag savings occur in formation flight. Whereas, a ratio above one reveals that the trailing aircraft produces a higher drag due to deviations to the normal flight trajectory.
In the third step, the method will be applied to a complete formation mission. It will be shown that the relative benefits of the follower decrease during the conduction of the mission due to the weight loss of both aircraft. Furthermore, it will be shown that the overall fuel savings of a formation strongly depend on the chosen parameters. Especially, the position in the vortex is the most influencing parameter.

4.1. Stationary loads during the formation

According to figure 2, the Airbus A330-200 belongs to the two most frequently used long haul aircraft families. Therefore, the formation of two A330-200 will be investigated in detail at first. Figure 9 shows the ratio of the induced drag in formation and in solo flight for different lateral and vertical separations. The formation flies at a flight Mach number of 0.82 and a flight altitude of 38000 ft. Both aircraft masses are in the middle between OME and MTOM, which is equal to 180328 kg. The range of k_y and k_z is set according to the studies of Ning, Flanzer and Kroo in figure 5.
Comparing the results with the studies of Ning et al. shows that the region with the highest drag reduction in AVL is at the height of the preceding aircraft and less inboard. Moreover, the drag savings in AVL are higher. While Ning et al. consider the movement of the trailing vortex due to wind gradients, turbulent gusts and interactions between the vortices, AVL assumes that the trailing legs of the horseshoe vortex filaments are parallel to the x-axis. This explains why the highest drag reduction is at the same level as the

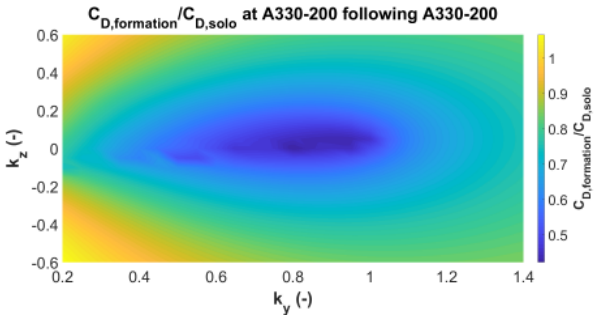

FIG 9. Change of induced drag at an A330-200 behind an A330-200 for different separation factors

leading aircraft. Moreover, the incorporation of the diffusion effects in the viscous decay of the vortex in the work of Ning et al. should lead to a more realistic result. In total, AVL estimates the reduction of the induced drag at the trailing aircraft approximately 50 % higher, which may be too optimistic.
Since the upwash velocity behind the leading aircraft is not constant, the lift distribution at the wing of the trailing aircraft is asymmetric. This leads to a induced roll moment, which is presented in figure 10 for the same flight conditions as in figure 9.
The figure points out that the highest drag reduction

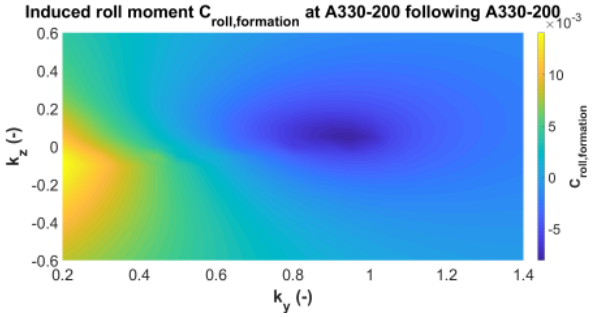

FIG 10. Induced roll moment at an A330-200 behind an A330-200 for different separation factors

is linked to the highest roll moment, because the highest upwash velocitiy leads to the highest reduction of the induced drag.
In the following studies, only five different values for each input parameter in tab:InputParameters are considered. A higher number of different values would lead to more than 10000 different combinations, which require a high computation time of over one day per formation pair, even on high performance computer clusters. The lateral and vertical separation factors are taken from the position with the highest drag reduction in figure 9. Hence the lateral separation factor k_y is set to 0.8 and the vertical separation factor k_z is set to zero. Figure 11 shows the drag saving potential for different altitudes and Mach numbers. The aircraft masses of the leading and the trailing aircraft are again set to 180328 kg. The highest drag reduction occurs for low Mach numbers and high altitudes and decreases for higher Mach numbers and lower altitudes. This can be explained by the different up wash velocities behind the leading

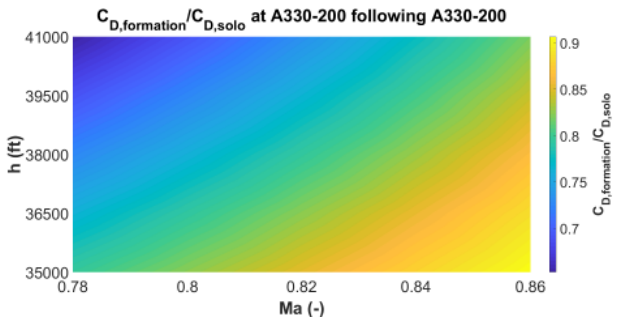

FIG 11. Drag savings at an A330-200 behind an A330-200 for different Mach numbers and altitudes

aircraft. For lower Mach numbers and higher altitudes the dynamic pressure q decreases, which requires a larger lift coefficient $C_{L,Leader}$ at a constant wing surface S to keep the aircraft at the same altitude.

$$C_{L,Leader} = F_z/(q \cdot S) \tag{2}$$

This leads to a larger pressure difference at the leading aircraft's wing and consequently a stronger upwind field.

During flight, the aircraft mass changes due to fuel consumption. Therefore, the aircraft mass is not considered as an optimization parameter. However, the different aircraft masses are important for the trajectory calculation.

Summarizing the results from AVL, table 4 presents the drag savings for all possible formation pairs with the aircraft types A330-200, A350-900, B777-200 and B787-8. The formations always fly at a Mach number of 0.78 and a flight altitude of 35000 ft. The aircraft mass is in the middle between OME and MTOM. The separation factors are again set to $k_y = 0.8$ and $k_z = 0$.

The highest drag reduction can be achieved,

		Leading aircraft			
		A330-200	A350-900	B777-200	B787-8
Trailing aircraft	A330-200	0.80	0.75	0.79	0.81
	A350-900	0.96	0.92	0.95	0.96
	B777-200	0.83	0.79	0.82	0.84
	B787-8	0.81	0.78	0.81	0.82

TAB 4. $C_{D,formation}/C_{D,ref}$ **for different formation pairs**

when an Airbus A330-200 flies behind an A350-900, whereas the lowest drag reduction can be observed, when the two aircraft switch their position in the formation. Overall, a drag reduction between 25% and 4% occur in the formation flight.

Considering the aircraft masses in table 5, the A350-900 has the greatest mass of 213405 kg and the A330-200 with 180328 kg is close to the lower

Aircraft type	Aircraft mass (kg)
A330-200	180328
A350-900	213406
B777-200	191042
B787-8	174248

TAB 5. Mass of considered aircraft types

limit. A high leading aircraft mass and a low trailing aircraft mass seem to be suitable to achieve a high drag reduction. A heavier aircraft produces more upwind in the trailing flow, which has the greatest impact for a light trailing aircraft. The reason for the lower drag reduction at the B787-8 compared to the A330-200 as the following aircraft may be the better aerodynamic performance and the lower total drag coefficient of the B787-8 in solo flight, which is estimated to 0.01899. In comparison, the A330-200 has a total drag coefficient of 0.02046.

4.2. Dynamic flight simulation

The most frequently used long haul aircraft family is the B777. Hence the formation flight of two Boeing B777-200 is investigated in the flight dynamic simulation. The simulation calculates the motion of the trailing aircraft for the same initial flight conditions (velocity, altitude, leading and trailing aircraft mass) as in AVL. In addition, three different gust and turbulence levels shall estimate the effect of atmospheric disturbances on the drag savings.

As an example, the initial flight conditions of table 6 are further analyzed. Due to the induced rolling

Ma	0.82
h(ft)	43000
m_{leader}(kg)	172000
$m_{follower}$(kg)	172000
Gust level / Turbulence level	2

TAB 6. Initial flight condition of the flight simulation

moment, which was presented in figure 10, and the atmospheric disturbances, the autopilot function in JSBSim has to compensate the external loads on the trailing aircraft and minimize the deviations from the optimum lateral and vertical position in the trailing wake. The estimated coefficients of the PID controllers of the B777-200 are determined according to chapter 3.2 and listed in table 7.

The effect of the autopilot on the flight altitude is shown in figure 12 for a simulation time of 500 seconds.

Without the autopilot, the trailing aircraft rises and sinks between +1000 ft and -3000 ft with regards to the initial altitude. The reason for the changing altitude can be explained by the different drag values in the look-up tables from AVL. When the aircraft

	PID 1	PID 2	PID 3
K_P	$1.496 * 10^-3$	21.96	$-6.886 * 10^-5$
K_I	$9.163 * 10^-8$	22.875	$-3.146 * 10^-6$
K_P	$4.034 * 10^-3$	3.689	$-1.554 * 10^-4$

TAB 7. PID control coefficients

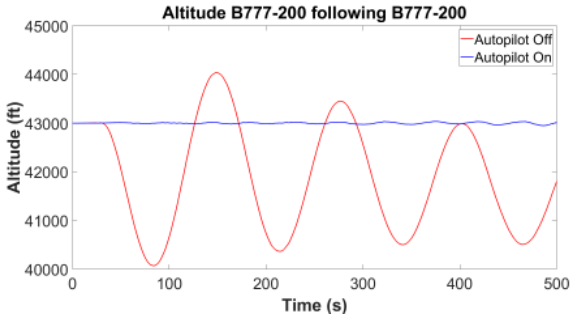

FIG 12. Altitude of the following Boeing B777-200

moves inside the leading aircraft vortex, steep vertical velocity gradients occur. These change the induced drag. At a constant thrust of the aircraft, the different drag changes the flight velocity of the aircraft. Assuming a constant lift coefficient, the lift of the aircraft changes proportionally with the flight velocity. Thus the varying flight velocity leads to different altitudes. The positive effect of the autopilot can be seen, as the altitude varies only between +/- 50 ft with an activated autopilot. Beside the altitude, the lateral separation distance between the leader and the follower changes according to figure 13.

The lateral distance between the two aircraft in-

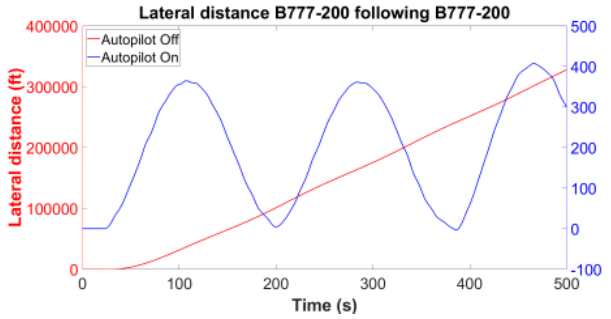

FIG 13. Lateral separation of the following Boeing B777-200 to the leader

creases to 300000 ft, if the autopilot is switched off (red curve). This seems to be not realistic and may be owing to a too low estimation of the roll stability in the program DATCOM+ Pro. When the asymmetric lift distribution in the vortex creates a roll moment, no counteracting moment is generated. As mentioned in chapter 3.2, the difficult determination of the dynamic coefficients in transonic flow may be the reason for this behavior. However, the implemented autopilot is able to reduce the lateral separation below 400 ft (blue curve).

Although the autopilot is able to reduce the separation between the formation pairs, the region for drag savings in figure 9 ranges vertically and laterally only over approximately $0.8 * (b_{trailing}/2)$, which is 160 ft. Therefore, the autopilot is not able to keep the trailing aircraft in the desired region to reduce drag over the whole simulation time. Hence, the averaged drag savings over a period of 300 seconds is below ten percent.

Investigations about different turbulence and gust levels have shown that the gust level has less impact on the change of drag than the turbulence level, which may be caused by the variing amplitude and direction of the wind vector in turbulent air. Table 8 points out that a significant decrease of the drag reduction occurs at a turbulence level of three. All other parameters were set according to table 6.

Gust level	Turbulence Level	$C_D/C_{D,ref}$
2	0	0.914
2	1	0.914
2	2	0.920
2	3	0.955

TAB 8. Influence of different turbulence levels on the drag savings

4.3. Trajectory calculation

During the trajectory calculation, the reduced thrust of the follower is accounted for by interpolation from the BDD and DRD. The thereby reduced fuel flow results in a reduced overall fuel consumption of the follower. For the leader no reduced fuel flow is obtained. Therefore, the leader might even use more fuel compared to the solo mission due to a necessary detour or a sub optimal operating point. The overall formation benefits are positive, if the follower's gains compensate the leader's losses. Additionally to the benefits of the follower, the reduced fuel consumption even increases the fuel savings as less fuel needs to be carried for the mission. As the trajectory calculation optimizes the block fuel mass needed for a mission, these so called fuel- for- fuel effects are included in the overall benefits. The relative benefits λ_f and absolute benefits Δm_{Bf} are determined by calculating the difference of the required block fuel mass m_B of the AWSE missions (index awse) to the according reference missions (index ref).

$$\lambda_f = \frac{\Delta m_{Bf}}{m_{Bf,ref}} = \frac{\sum m_{B,ref} - \sum m_{B,awse}}{\sum m_{B,ref}} \quad (3)$$

As the benefits of an AWSE mission depend on the position of the follower in the leaders vortex, it is important to know whether this position can be subject to optimization in order to achieve the maximum benefits of a formation. Therefore, the dependencies of the benefits on the lateral separation were calculated for a set of representative AWSE missions and a vertical separation factor of zero.

Figure 14 shows the relative benefits of a selection

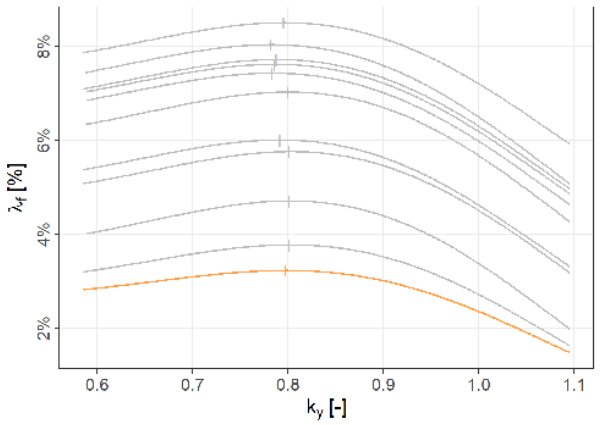

FIG 14. Relative fuel benefits for different missions and lateral separation factors

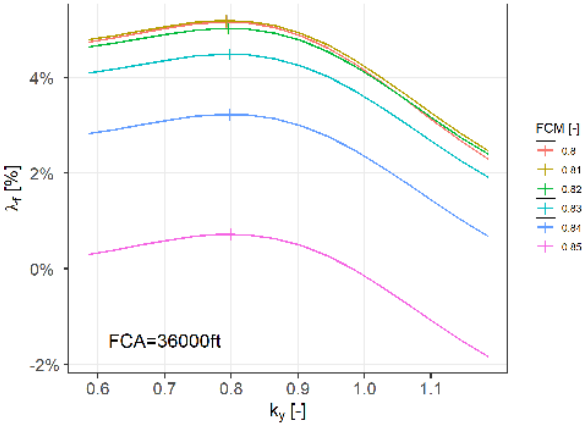

FIG 16. Relative fuel benefits for different Mach numbers and lateral separation factors

of example missions (grey) as well as for the example mission presented in [22] with a formation altitude of 36000 ft and a formation Mach number of 0.84 (orange) over the lateral separation factor k_y. Generally, the shapes of the curves are comparable, but it can be observed that, depending on the mission, the values of k_y, that lead to maximum benefits, are shifted in the range between 0.78 and 0.8 meaning the tip of the follower's wing can be assumed to be close to the vortex core of the leader.

Figure 15 and 16 show the relative formation benefits

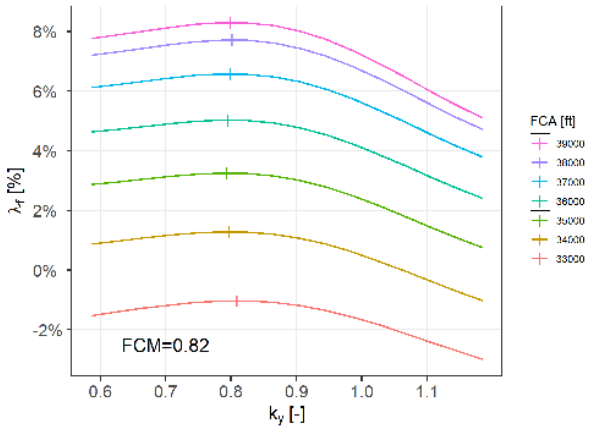

FIG 15. Relative fuel benefits for different altitudes and lateral separation factors

λ_f for the example mission presented in [22] over k_y for different FCM (Formation Cruise Mach) and FCA (Formation Cruise Altitude) values. A strong dependency of the benefits can be observed, which increase with higher FCA and decrease with higher FCM. However, the shift of k_y yielding the maximum benefits for the different FCM and FCA values is low averaging out at about $k_t = 0.799$ for FCA variation and 0.796 for FCM variation.

As the position of the wingtip of the follower close to the vortex core of the leader is not favorable in an AWSE flight, a position more outside of the vortex core (for example $k_t > 0.9$) will be selected. In this case the above results demonstrate that the tip spacing is not subject to optimization in order to maximize the formation benefits at mission level. However, further investigations of multiple formation route geometries and settings as well as the creation of more detailed aerodynamic databases are necessary to assess the dependencies of the formation benefits on the parameters more thoroughly.

4.4. Influence of the parameters on the fuel savings

The overall benefits of a formation strongly depend on the formation parameters given by the participating aircraft types, the aircraft masses, the altitude and speed of the formation as well as on the position of the follower in the vortex of the leader.

The investigations have shown that the cruise speed in formation should be low, whereas the cruise altitude should be as high as possible. Combining a heavy leading aircraft and a light trailing aircraft yields the greatest drag reduction. However, the fuel consumption and the lower aircraft mass towards the end of the mission decreases the benefits. Older aircraft families benefit the most, when they are flying at the trailing position. Furthermore, atmospheric disturbances and induced loads of the leading aircraft reduce the drag savings below ten percent. Strong turbulence (level three) reduce the drag savings even below 5 percent and can lead to uncontrollable aircraft behaviors.

5. CONCLUSION

This paper investigated the benefits of air wake surfing for efficiency (AWSE) for long haul commercial aircraft with a design range of over 5000 nm. Based on the numbers of deliveries and orders four different aircraft types (A330-200, A350-900, B777-200, B787-8) have been considered to evaluate the effects of different flight conditions, atmospheric disturbances and aircraft types on the potential savings.

For the stationary state, a vortex lattice method determines the induced loads for different flight conditions and separation distances between the leading and the trailing aircraft. Compared to existing literature on extended formation flight with a stream wise separation of more than five spans, the vortex lattice method overestimates the drag reduction about 50%, which may be linked to the simplified vortex propagation in the vortex lattice method. However, the method allows a comparison between different formation pairs and an analysis of the influence of the different formation flight parameters. Between the lower limit with a minimum cruise Mach number of 0.78 and a cruise altitude of 35000 ft and the corresponding maximum operating limits the benefits for AWSE varied between 25%. The results showed that a low speed and high altitude is beneficial for high savings. Furthermore, different combinations of the four most frequently operated long haul aircraft families (A330, A350, B777, B787) lead to drag reductions between 4% and 25%. A heavy leading aircraft provided the highest benefits.
In the flight dynamic simulation of the formation flight, the average total drag at the trailing aircraft during five minutes of formation flight was calculated. If the autopilot is not activated, a very high lateral displacement of the trailing aircraft occurred. This is owing to the difficult estimation of the flight dynamic of the trailing aircraft in a transonic flow. The simplified autopilot structure was not able to keep the aircraft at the desired region of high drag reductions for a long time, which lead to a lower drag reduction of ten percent. Besides that, severe turbulence caused a significant decrease of the drag reduction. Better results are expected with a more realistic autopilot system.
Considering the whole mission, the trajectory calculation showed that the fuel consumption during the mission decreases the aircraft weight and the AWSE benefits towards the end of the mission. Furthermore, the advantages of formation flying are unequally distributed. On the one hand the lower fuel consumption of the trailing aircraft lead to a lower take-off mass, whereas on the other hand the leading aircraft may need extra fuel to perform the formation flight.

Contact address:

clemens.zumegen@ilr.rwth-aachen.de

References

[1] International Council on Clean Transportation. CO2 emissions from commercial aviation, 2018, 2019.

[2] International Air Transport Association. Fact sheet: CORSIA, 2020.

[3] Andre Koloschin and Nicolas Fezans. Flight Physics of Fuel-Saving Formation Flight. In American Institute of Aeronautics and Astronautics, editor, *AIAA SciTech 2020 Forum*, 2020.

[4] Markus Beukenberg and Dietrich Hummel. Aerodynamics, performance and control of airplanes in formation flight. In *17th Congress of the International Council of the Aeronautical Sciences*, volume 17, pages 1777–1794, 1990.

[5] Joe Pahle, Dave Berger, Mike Venti, Chris Duggan, Jim Faber, and Kyle Cardinal. An Initial Flight Investigation of Formation Flight for Drag Reduction on the C-17 Aircraft. In American Institute of Aeronautics and Astronautics, editor, *AIAA Atmospheric Flight Mechanics Conference*, pages 1–13, 2012. DOI: 10.2514/6.2012-4802.

[6] Airliners.de. Airbus will Flugzeuge im Schwarm fliegen lassen, 2019.

[7] DVB Bank SE Aviation Research. An Overview of Commercial Aircraft 2018 - 2019, 2017.

[8] A. Betz. Behavior of vortex systems, 1933.

[9] Coleman duP. Donaldson. A brief review of the aircraft trailing vortex problem, 1971.

[10] Andrew S. Ning, Tristan C. Flanzer, and Ilan M. Kroo. Aerodynamic Performance of Extended Formation Flight. In American Institute of Aeronautics and Astronautics, editor, *48th AIAA Aerospace Sciences Meeting including the New Horizons Forum and Aerospace Exposition*, pages 1–20, 2010. DOI: 10.2514/6.2010-1240.

[11] D. P. Delisi, G. C. Greene, R. E. Robins, D. C. Vicroy, and F. Y. Wang. Aircraft Wake Vortex Core Size Measurements. In American Institute of Aeronautics and Astronautics, editor, *21st Applied Aerodynamics Conference*, 2003.

[12] Kristof Risse, Eckhard Anton, Tim Lammering, Katharina Franz, and Ralf Hoernschemeyer. An Integrated Environment for Preliminary Aircraft Design and Optimization. In American Institute of Aeronautics and Astronautics, editor, *53rd AIAA/ASME/ASCE/AHS/ASC Structures, Structural Dynamics and Materials Conference: SciTech 2012*, volume AIAA 2012-1675. AIAA, 2012. DOI: 10.2514/6.2012-1675.

[13] Yaolong Liu. *Investigation on the Benefit and Feasibility of Applying Formation Flight to Civil Transport Aircraft*. Dissertation, RWTH Aachen University, Aachen, Germany, 2016.

[14] M. Drela and H. Youngren. Athena vortex lattice - avl 3.36 user primer. 2017.

[15] Simon Hoffmann and Rainer Lienhart. *OpenMP: Eine Einführung in die parallele Programmierung mit C/C++*. Springer, Berlin, Heidelberg, 2008. ISBN: 978-3-540-73122-1.

[16] R. D. Finck. USAF STABILITY AND CONTROL DATCOM, 1978.

[17] Clemens Zumegen and Eike Stumpf. Flight behavior of long-haul commercial aircraft in formation flight. In Air Transport Research Society, editor, *23rd ATRS World Conference*, 2019.

[18] David J. Moorhouse and Robert J. Woodcock. *Background information and user guide for MIL-F-8785C, military specification - flying qualities of piloted airplanes*. US Government Printing Office, Ohio, 1982.

[19] Kun Li Chien, J. A. Hrones, and J. B. Reswick. On the automatic control of the generalized passive systems". *Transactions of the American Society of Mechanical Engineers*, (74):175–185, 1952.

[20] Florian Linke. Trajectory Calculation Module (TCM) - Tool Description and Validation, 2014.

[21] B. Lührs, Florian Linke, and V. Gollnick. Erweiterung eines Trajektorienrechners zur Nutzung meteorologischer Daten für die Optimierung von Flugzeugtrajektorien. In Deutsche Gesellschaft für Luft- und Raumfahrt, editor, *Deutscher Luft- und Raumfahrtkongress*, 2014.

[22] Tobias Marks, Clemens Zumegen, Volker Gollnick, and Eike Stumpf. Assessing formation flight benefits on trajectory level including turbulence and gust. In Italian Association of Aeronautics and Astronautics, editor, *AIDAA XXV International Congress*, 2019.